

An algebraic expression of stable inversion for nonminimum phase systems and its applications [★]

Takuya Sogo ^{*}

^{*} Chubu University, Aichi 487-8501, Japan
(Tel: +81-568-51-9771; e-mail: sogo@isc.chubu.ac.jp).

Abstract: This paper proposes an algebraic expression of noncausal stable inversion based on the two-sided Laplace transform, which is a classic mathematical tool but has not been used very much in the field of control engineering. This expression brings an advantage that computing of stable inversion is reduced to simulation of the response of the plant and the reverse of time horizon without solving the boundary value problem of state-space equations as the conventional definition of stable inversion. An illustrative example demonstrates that this approach is useful to reduce the load of the programming for a search algorithm to determine the shape of a transition trajectory under the constraint of input saturation. As another application of the proposed expression, developed is a method of iterative learning control to obtain stable inversion for infinite dimensional systems. An experiment to apply the iterative learning control to tip control of a flexible arm is reported to demonstrate the effectiveness of the method.

Keywords: Stable inversion, Input design, Iterative learning control, Dynamic inversion, Nonminimum phase systems, Feedforward control, Preview control, Input shaping, Laplace transforms

1. INTRODUCTION

System inversion plays crucial roles in many control applications such as perfect tracking, transient response shaping, disturbance attenuation, and noise cancellation. For example, consider shaping the transient response of a plant $G(s)$. Then, if $1/G(s)$ is stable, one can employ $F(s) = M(s)/G(s)$ as a prefilter of $G(s)$, where $M(s)$ is a model that has a desired response. If $G(s)$ is a nonminimum phase system or equivalently $1/G(s)$ is unstable, $F(s) = M(s)/G(s)$ cannot be used as a prefilter. However it was proposed to substitute the optimal function of the model matching problem

$$\min \|G(s)F(s) - M(s)\|_{\infty} \quad F(s) \in RH_{\infty} \quad (1)$$

for a prefilter instead of the unstable $F(s) = M(s)/G(s)$. This approach has an advantage that both prefilters and feedback controllers can be designed in the same framework of H_{∞} optimization (Limebeer et al. (1993)). It is recognized that feedback controller design based on the transfer function is very effective from the viewpoint of robustness or sensitivity design. However, effectiveness of the prefilter designed by the aforementioned approach is controversial from the viewpoint of response shaping.

On the other hand, noncausal stable inversion technique was proposed in order to calculate a bounded input which achieves perfect tracking even if $1/G(s)$ is unstable, equivalently, $M(s)/G(s) \notin RH_{\infty}$. (Devasia et al. (1996); Zou and

[★] This work was supported in part by a Grant-in-Aid for Scientific Research (C) No.18560444 from the Japan Society for the Promotion of Science and a grant from the High-Tech Research Center Establishment Project from the Ministry of Education, Culture, Sports, Science and Technology, Japan.

Devasia (1999); Hunt et al. (1996)). This technique utilizes noncausal or preview information of desired trajectories in order to generate bounded input profiles. In most of the work reported so far, the calculation of stable inversion is based on solving the boundary value problem of the inverted state-space equations. This means that transfer functions are necessarily transformed into state-space representations to design stable inversion even if feedback controller design is based on transfer functions which are common in control engineering.

In order to improve this inconvenience, this paper introduces the two-sided Laplace transform to express stable inversion and its calculation simply as unstable transfer function $1/G(s)$ and noncausal convolution, respectively. It will be shown that the proposed transfer-function expression of inversion is actually equivalent to the conventional stable inversion expressed by state-space representations; this simplifies computing the input profile for stable inversion. It will be demonstrated that stable inversion based on the transfer-function expression can be applied to infinite dimensional systems. This will be illustrated by an example of iterative learning control applied to tip positioning of a flexible arm.

In this paper, we use following notations: For $f(t) : (-\infty, +\infty) \rightarrow R$, norms of $f(t)$ are defined as $\|f(t)\|_{\infty} := \text{ess sup}_{t \in (-\infty, +\infty)} |f(t)|$, $\|f(t)\|_1 := \int_{-\infty}^{+\infty} |f(t)| dt$ and $\|f(t)\|_2 := \int_{-\infty}^{+\infty} |f(t)|^2 dt$. Spaces of functions which have bounded $\|\cdot\|_1$, $\|\cdot\|_2$ and $\|\cdot\|_{\infty}$ norms are denoted by L_1 , L_2 and L_{∞} , respectively. For $F(s) : C \rightarrow C$, norms of $F(s)$

are defined as $\|F(s)\|_\infty = \text{ess sup}_{\omega \in (-\infty, +\infty)} |F(j\omega)|$ and $\|F(s)\|_2 := \int_{-\infty}^{+\infty} |F(j\omega)|^2 d\omega$.

2. STABLE INVERSION FOR LTI SYSTEMS

Consider a plant

$$G(s) = \frac{c_0 s^m + \dots + c_{m-1} s + c_m}{s^n + a_1 s^{n-1} + \dots + a_{n-1} s + a_n} \quad (2)$$

with the controllable canonical form of the state-space representation (A, B, C) . We assume that all poles of $G(s)$ or eigenvalues of A are in the left half plane. Then Silverman's inversion (Silverman (1969)) of the system is expressed as

$$\begin{pmatrix} \dot{x}_{n-m+1} \\ \vdots \\ \dot{x}_{n-1} \\ \dot{x}_n \end{pmatrix} = \Phi \begin{pmatrix} x_{n-m+1} \\ \vdots \\ x_{n-1} \\ x_n \end{pmatrix} + \begin{pmatrix} 0 \\ \vdots \\ 0 \\ 1/c_0 \end{pmatrix} y^{(n-m)} \quad (3)$$

$$u = \Gamma \begin{pmatrix} x_{n-m+1} \\ \vdots \\ x_{n-1} \\ x_n \end{pmatrix} + \Lambda \begin{pmatrix} y \\ \vdots \\ y^{(n-m-1)} \\ y^{(n-m)} \end{pmatrix} \quad (4)$$

where $y^{(k)} = d^k y / dt^k$, equivalently

$$\begin{aligned} 1/G(s) &= (s^{n-m} + \bar{a}_1 s^{n-m-1} + \dots + \bar{a}_{n-m}) / c_0 \\ &+ \frac{\bar{a}_{n-m+1} s^{m-1} + \dots + \bar{a}_n}{c_0 s^m + c_1 s^{m-1} + \dots + c_m} \end{aligned} \quad (5)$$

If $G(s)$ is a nonminimum phase system, Φ has eigenvalues in the right half plane and the solution of the initial value problem of (3) is unbounded. This means that the input to achieve perfect tracking to an output trajectory y_d is unbounded in the causal framework. However, if the constraint of causality is not imposed on (3), there exists an input to achieve perfect tracking for a class of output trajectories.

Proposition 1. [Devasia et al. (1996); Hunt et al. (1996)] Assume that

$$y_d^{(i)} \in L_1 \cap L_\infty \quad (i = 0, 1, \dots, n-m) \quad (6)$$

and $G(s)$ has no zero on the imaginary axis. Then, there exist bounded $x_d(t)$ and $u_d(t)$ such that

$$\dot{x}_d = Ax_d + Bu_d \quad (7)$$

$$y_d = Cx_d \quad (8)$$

and

$$u_d(t) \rightarrow 0, x_d(t) \rightarrow 0 \quad \text{as } t \rightarrow \pm\infty \quad (9)$$

□

Functions $x_d(t)$ and $u_d(t)$ given in Proposition 1 are obtained by solving the differential equation (3) under the boundary condition (9). Calculating the bounded input $u_d(t)$ defined by Proposition 1 requires the following steps:

- (1) transform of the transfer function into the state-space equation
- (2) inversion of the state-space equation
- (3) solving of the boundary value problem

In order to reduce these steps, we develop a simple method based on transfer functions in the next section.

3. ALGEBRAIC EXPRESSION OF STABLE INVERSION

Since all elements in feedback control systems are on-line and causal, the one-sided Laplace transform is widely used to analyze control systems algebraically. In order to import noncausal elements into the same framework, we introduce the two-sided Laplace transform (Van der Pol and Bremmer (1987); Papoulis (1962)), which is a classic mathematical tool but has not been very common in the field of control engineering¹.

For a function $g(t)$ defined on the infinite time horizon, the two-sided Laplace transform is defined as

$$\mathcal{L}[g(t)](s) = G(s) := \int_{-\infty}^{+\infty} e^{-st} g(t) dt \quad (10)$$

where the region of convergence is the strip $\{s; \gamma_1 < \text{Re}(s) < \gamma_2\}$ (Van der Pol and Bremmer (1987); Papoulis (1962)). It should be noted that

$$\mathcal{L}[g'(t)](s) = sG(s) \quad (11)$$

$$\mathcal{L}\left[\int_{-\infty}^t g(\tau) d\tau\right](s) = \frac{G(s)}{s} \quad (12)$$

$$\mathcal{L}\left[\int_{-\infty}^{+\infty} g(t-\tau) f(\tau) d\tau\right](s) = G(s)F(s) \quad (13)$$

where $F(s) = \mathcal{L}[f(t)](s)$. The inverse transform is expressed by

$$\begin{aligned} \mathcal{L}^{-1}[G(s)](t) &= g(t) = \frac{1}{2\pi j} \int_{\alpha-j\infty}^{\alpha+j\infty} e^{st} G(s) ds \\ &= \begin{cases} \sum_{\text{Re}(p_n) < \alpha} \text{Res}(e^{st} G(s), p_n) & t \geq 0 \\ \sum_{\text{Re}(p_m) > \alpha} \text{Res}(-e^{st} G(s), p_m) & t < 0 \end{cases} \end{aligned} \quad (14)$$

where $\{p_n\}$ and $\{p_m\}$ denote the sets of poles of $G(s)$ which are in the left and right half plane of the vertical line $s = \alpha$, respectively.

The next theorem shows that inversion of the transfer function based on the two-sided Laplace transform is actually equivalent to stable inversion defined in Proposition 1.

Theorem 2. Assume that $y_d^{(i)} \in L_1 \cap L_\infty$ ($i = 0, 1, \dots, n-m$) and $G(s)$ has no zero on the imaginary axis. Functions u_d and x_d satisfying (7), (8) and (9) are expressed by

$$u_d(t) = \mathcal{L}^{-1}[1/G(s) \cdot Y_d(s)] \quad (15)$$

$$x_d(t) = \mathcal{L}^{-1}[(sI - A)^{-1} B U_d(s)] \quad (16)$$

where $Y_d(s) = \mathcal{L}[y_d]$ and $U_d(s) = \mathcal{L}[u_d]$. □

Proof: From the assumption on y_d , we have

$$\mathcal{L}^{-1}[(s^{n-m} + \bar{a}_1 s^{n-m-1} + \dots + \bar{a}_{n-m}) Y_d(s)] \in L_1 \cap L_\infty \quad (17)$$

Since $G(s)$ has no zero on the imaginary axis, α of (14) for the fraction term of (5) can be chosen as 0. This implies

$$\mathcal{L}^{-1}\left[\frac{\bar{a}_{n-m+1} s^{m-1} + \dots + \bar{a}_n}{c_0 s^m + c_1 s^{m-1} + \dots + c_m}\right] \in L_1 \cap L_\infty \quad (18)$$

¹ As far as the author knows, an application to identification of systems with delay was reported in the field of control engineering (Kachanov and Khrolovich (1993))

moreover

$$\mathcal{L}^{-1} \left[\frac{\bar{a}_{n-m+1}s^{m-1} + \dots + \bar{a}_n}{c_0s^m + c_1s^{m-1} + \dots + c_m} Y_d(s) \right] \in L_1 \cap L_\infty \quad (19)$$

From (17) and (19), u_d defined by (15) satisfies $u_d(t) \in L_1 \cap L_\infty$. Since all eigenvalues of A are in the left half plane, $u_d(t) \in L_1 \cap L_\infty$ implies $x_d(t) \in L_1 \cap L_\infty$ which leads to (9).

From the definition of $G(s)$ and (A, B, C) , u_d and x_d defined by (15) and (16) satisfies (7) and (8). This completes the proof. \square

Remark 3. It should be noted that the input profile (15) is defined even though $y_d^{(i)} \notin L_1 \cap L_\infty$. (See Example 1 below) This implies that the inversion based on the two-sided Laplace transform generalizes the stable inversion defined by Proposition 1.

The next corollary shows that the noncausal convolution for (15) can be substituted by the ordinary causal convolution for two stable systems with the reverse of the time horizon. In the following discussion, $\bar{\mathcal{L}}$ denotes the conventional one-sided Laplace transform, namely

$$\bar{\mathcal{L}}[g(t)](s) = G(s) := \int_0^{+\infty} e^{-st}g(t)dt \quad (20)$$

Corollary 4. Assume that $y_d^{(i)} \in L_1 \cap L_\infty$ ($i = 0, 1, \dots, n-m$) and $G(s)$ has no zero on the imaginary axis. Let

$$1/G(s) = (s^{n-m} + \bar{a}_1s^{n-m-1} + \dots + \bar{a}_{n-m})/c_0 + F_l(s) \cdot F_r(s) \quad (21)$$

where $F_l(s)$ and $F_r(s)$ are proper transfer functions all poles of which are in the left and right half plane, respectively. Then $u_d(t)$ defined by (15) is expressed by

$$u_d(t) = (y_d^{n-m}(t) + \bar{a}_1y_d^{n-m-1}(t) + \dots + \bar{a}_{n-m}y_d(t))/c_0 + \int_{-\infty}^t f_l(t-\tau)v(\tau)d\tau \quad (22)$$

$$v(t) = \int_{-\infty}^\sigma f_r(\sigma-\tau)y_d(-\tau)d\tau \Big|_{\sigma=-t} \quad (23)$$

where

$$f_l(t) = \bar{\mathcal{L}}^{-1}[F_l(s)] \quad (24)$$

$$f_r(t) = \bar{\mathcal{L}}^{-1}[F_r(-s)] \quad (25)$$

\square

Proof: From (14) with $\alpha = 0$, we have

$$\mathcal{L}^{-1}[F_l(s)] = \begin{cases} \sum_n \text{Res}(e^{st}F_l(s), p_n) & \text{if } t \geq 0 \\ 0 & \text{if } t < 0 \end{cases} \quad (26)$$

$$= \bar{\mathcal{L}}^{-1}[F_l(s)] = f_l(t) \quad (27)$$

$$\mathcal{L}^{-1}[F_r(-s)] = \begin{cases} \sum_m \text{Res}(e^{st}F_r(-s), -p_m) & \text{if } t \geq 0 \\ 0 & \text{if } t < 0 \end{cases} \quad (28)$$

$$= \bar{\mathcal{L}}^{-1}[F_r(-s)] = f_r(t) \quad (29)$$

and

$$\mathcal{L}^{-1}[F_r(s)] = -\frac{1}{2\pi j} \int_{+j\infty}^{-j\infty} e^{-st}F_r(-s)ds \quad (30)$$

$$= \begin{cases} 0 & \text{if } t \geq 0 \\ -\sum_m \text{Res}(-e^{-st}F_r(-s), -p_m) & \text{if } t < 0 \end{cases} \quad (31)$$

$$= f_r(-t) \quad (32)$$

These equalities with (11) and (13) imply (22) and

$$v(t) = \int_t^{+\infty} f_r(-(t-\tau))y_d(\tau)d\tau \quad (33)$$

which leads to (23). \square

From Corollary 4, one can obtain the input profile based on the stable inversion by the following steps:

- (1) decomposition of the proper part of the inverted transfer function into the cascade connection of the stable and antistable part
- (2) computation of the causal convolution or the solution of the initial value problem with reversing the time horizon

Example 1. Consider a nonminimum phase system

$$G(s) = \frac{(s+4)(3-s)}{s^3 + 2s^2 + 3s + 4} \quad (34)$$

and a function

$$y_d(t) = \begin{cases} 0 & \text{if } t < 0 \\ \frac{e^{-\frac{1}{t^3}}}{e^{-\frac{1}{t^3}} + e^{-\frac{1}{1-t^3}}} & \text{if } 0 \leq t \leq 3 \\ 1 & \text{if } t > 3 \end{cases} \quad (35)$$

as the desired output trajectory of (34); the function (35) is a C^∞ function which is monotonously increasing from 0 to 1 and $Y_d(s) = \mathcal{L}[y_d(t)]$ exists for $\{s; 0 < \text{Re}(s)\}$. To calculate the input that achieves perfect tracking to (35), express $1/G(s)$ as

$$\frac{1}{G(s)} = -s - 1 + \frac{4s + 16}{s + 4} \cdot \frac{1}{3 - s} \quad (36)$$

then one can see that $\mathcal{L}^{-1}[1/G(s) \cdot Y_d(s)]$ is well-defined and bounded since $y_d(t) \in C^\infty$ and $\mathcal{L}^{-1}[(4s + 16)/\{(s + 4)(3 - s)\}Y_d(s)] \in L_\infty$ with $\{s; 0 < \text{Re}(s) < 3\}$.

The input profile $u_d(t) = \mathcal{L}^{-1}[1/G(s) \cdot Y_d(s)]$ is computed by (23) and (22) with

$$F_l(s) = \frac{4s + 16}{s + 4}, F_r(-s) = \frac{1}{s + 3} \quad (37)$$

which can be easily computed by a standard tool for numerical simulation (e.g. `lsim` command in MATLAB). It should be noted that the convolution over the infinite time horizon for (35) can be approximated by a convolution over a sufficiently long time interval with truncation. Fig. 1 shows the computed u_d and its response.

Remark 5. For MIMO systems, algebraic expression of stable inversion corresponds to the inversion of transfer function matrix. The time-domain calculation proposed in Corollary 4 can be applied to each element of the transfer function matrix.

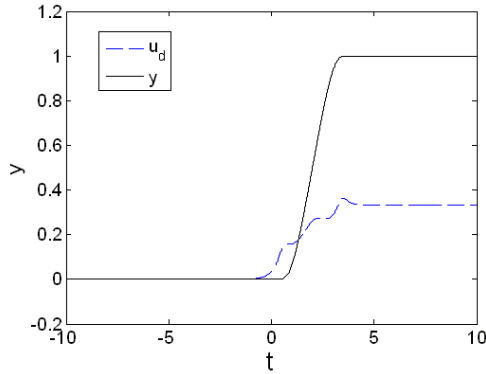


Fig. 1. The input profile and its response for Example 1

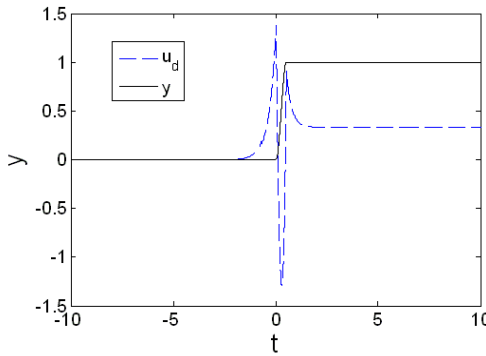


Fig. 2. The input profile with $T = 1$ and its response for Example 2

4. APPLICATIONS OF TRANSFER FUNCTION EXPRESSION OF STABLE INVERSION

In the preceding section, suggested was that the algebraic expression of stable inversion has advantages in computing and the range of applications. This section presents two practical examples.

4.1 Application to optimization of a transition trajectory under input constraint

In many control applications, of importance is shaping a trajectory that achieves a fast monotonous transition between two constant values under input saturation:

$$|u(t)| \leq u_{\max} \quad \text{for } t \in (-\infty, +\infty) \quad (38)$$

Example 2. Consider (34) with a C^1 function

$$y_d(t) = \begin{cases} 0 & \text{if } t < 0 \\ \frac{3!}{T^3} \sum_{i=0}^1 \frac{(-1)^{1-i}}{i!(1-i)!(3-i)} T^i t^{3-i} & \text{if } 0 \leq t \leq T \\ 1 & \text{if } t > T \end{cases} \quad (39)$$

as a desired trajectory where T is the time parameter of transition that affects the peak value of the input (Piazzi and Visioli (2005)). Fig. 2 shows the input profile $u_d(t)$ that achieves $y(t) = y_d(t)$ with $T = 1$. It was proven that if

$$u_{\max} \geq \frac{1}{|G(0)|} \quad (40)$$

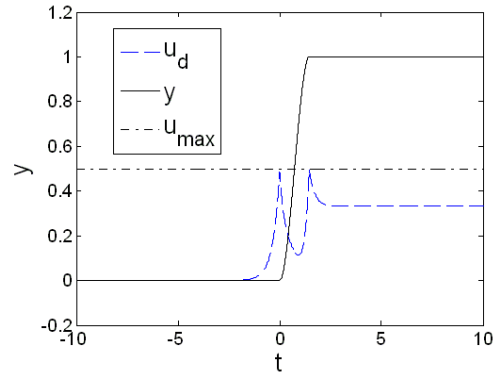


Fig. 3. The input profile satisfying the constraint and its response for Example 2

the feasible set $\{T\}$ for (38) is nonempty and there exists the minimum transition time T_{\min} under the constraint (Piazzi and Visioli (2005)). One can find T_{\min} practically by a bisection search algorithm with respect to T . It should be noted that Corollary 4 reduces the load of coding of the search algorithm since no explicit expression $u_d(t)$ for each $y_d(t)$ is required. For

$$u_{\max} = 0.5 \quad (41)$$

a value $T = 1.4609$ was found by a bisection search starting from the interval $[1, 2]$ for T . Fig. 3 shows the found input $u_d(t)$ and its response $y(t)$.

4.2 Application to an infinite dimensional system

The algebraic expression of stable inversion presented in Section 3 suggests that stable inversion is essentially applicable to infinite dimensional systems. It is, however, practically difficult to execute the computation given in Corollary 4 because of the difficulty of identification of the infinite-dimensional model. To circumvent this, we develop an iterative method to obtain the desired input profile without the decomposition of $1/G(s)$.

Theorem 6. Assume that there exists

$$\mathcal{L}^{-1}[1/G(s) \cdot Y_d(s)] \in L_1 \cap L_\infty \quad (42)$$

and $G(s)$ has no zeros on the imaginary axis and $G(j\omega) \rightarrow 0$ as $|\omega| \rightarrow \infty$. Let $y_d(t)$ be a desired output trajectory and $Y_d(s) = \mathcal{L}^{-1}[y_d(t)]$. Then, the sequence of input functions $\{U_k(s); k = 0, 1, \dots\}$ defined by

$$U_0(s) \equiv 0 \quad (43)$$

$$U_{k+1}(s) = U_k(s) - \alpha G(-s) \{G(s)U_k(s) - Y_d(s)\} \quad (44)$$

satisfies

$$\|U_k(s) - 1/G(s) \cdot Y_d(s)\|_2 \rightarrow 0 \quad \text{as } k \rightarrow \infty \quad (45)$$

where α is a constant satisfying $0 < \alpha < 1/\|G(s)\|_\infty^2$.

Proof: Let $E_k(s) = U_k(s) - 1/G(s) \cdot Y_d(s)$. Then we have $E_{k+1}(s) = (1 - \alpha G(-s)G(s))E_k(s)$ which leads to $E_{k+1}(j\omega) = (1 - \alpha|G(j\omega)|^2)E_k(j\omega)$ moreover $|E_k(j\omega)|^2 = (1 - \alpha|G(j\omega)|^2)^{2k}|E_0(j\omega)|^2$. Since $1 - \alpha|G(j\omega)|^2 < 1$ for $\omega \in (-\infty, +\infty)$, we have

$$\|E_k(s)\|_2^2 \leq \int_{-\Omega}^{+\Omega} (1 - \alpha|G(j\omega)|^2)^{2k} |E_0(j\omega)|^2 d\omega + \int_{\Omega < |\omega| \leq \infty} |E_0(j\omega)|^2 d\omega \quad (46)$$

for any positive Ω . Note that (42) implies $E_0(s) = -1/G(s) \cdot Y_d(s) \in L_2$. Then we have

$$\int_{\Omega < |\omega| \leq \infty} |E_0(j\omega)|^2 d\omega \rightarrow 0 \quad (47)$$

as $\Omega \rightarrow \infty$. Hence, for any given $\epsilon > 0$, there exist Ω and an positive integer N such that $\|E_k(s)\|_2^2 < \epsilon/2 + \epsilon/2$ for all $k > N$. This completes the proof. \square

The algorithm given in Theorem 6 is equivalent to a time-domain algorithm which requires only measuring of the response of the plant $G(s)$.

Corollary 7. Assume the same properties as Theorem 6 and all poles of $G(s)$ are in the left half plane. Then the sequence of inputs $\{u_k(t); k = 0, 1, \dots\}$ defined by

$$\eta_k(t) = \int_{-\infty}^t g(t-\tau)u_k(\tau)d\tau - y_d(t) \quad (48)$$

$$u_{k+1}(t) = u_k(t) - \alpha \int_{-\infty}^{\sigma} g(\sigma-\tau)\eta_k(-\tau)d\tau \Big|_{\sigma=-t} \quad (49)$$

satisfies

$$\|u_k(t) - \mathcal{L}^{-1}[1/G(s) \cdot Y_d(s)]\|_2 \rightarrow 0 \quad (50)$$

as $k \rightarrow \infty$.

Proof: The assumption of poles of $G(s)$ with (13) and (14) implies (48). Since all poles of $G(-s)$ are in the right half plane, (49) is obtained by the same discussion as the proof of Corollary 4. By the Parseval equality, (50) follows (45). \square

In contrast to the method in Corollary 4, there is no need of the decomposition of the inverted transfer function for the method given in Corollary 7. Moreover, all required integrations are the convolution for $G(s)$, which is obtained as the response of $G(s)$. This can be done experimentally on real plants without identifying a model of the plant. The iterative method presented in Corollary 4 is summarized as the following steps.

- (0) $k := 0; u_0(t) \equiv 0$
- (1) measure the response of $G(s)$ for the input $u_k(t)$ and record the error $\eta_k(t)$
- (2) measure the response of $G(s)$ for the time-reversed error $\eta_k(-t)$
- (3) update the input with the time-reversed response and the last input
- (4) $k := k + 1$ and go to (1)

Remark 8. The iterative method presented in Corollary 7 is actually a generalization of iterative learning control using adjoint systems which was proposed with state-space representations(Kinoshita et al. (2002)). Theorem 6 extends the applicable range of iterative learning control(Kinoshita et al. (2002); Markusson et al. (2001); Owens and Hätönen (2005); Moore (1993)).

Example 3. Consider tip control of a experimental flexible arm depicted in Fig. 4 (The length of the arm: $L = 3.0 \times 10^{-1}$ m, the moment of inertia of the arm including the hub: $I = 637.4 \times 10^{-6}$ Kg \cdot m²). The hub is directly driven by a DC motor; the rotational angle $\theta(t)$ [rad] with respect to the inertial reference frame is measured by a rotary encoder embedded in the motor. The deflection of the tip $w(L, t)$ with respect to the frame fixed on the hub is measured by an optical device on the hub, which senses the horizontal location of a light source attached to the

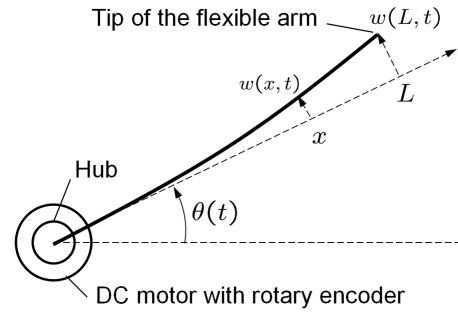


Fig. 4. experimental setup of the flexible arm

tip. Assuming that the deflection of the tip is sufficiently smaller than the length of the arm, we consider

$$y(t) = L\theta(t) + w(L, t) [m] \quad (51)$$

as the position of the tip. The dynamics of the motor is expressed by $T(s) = K_m/R \cdot V_{in}(s) - K_m^2/R \cdot \dot{\theta}(s)$ where $K_m = 7.67 \times 10^{-3}$ Nm/A and $R = 2.60\Omega$. Observations based on the Euler-Bernoulli model lead to transfer functions of the flexible arm as follows(Cannon and Schmitz (1984)):

$$\frac{\dot{\theta}(s)}{T(s)} = \frac{1}{Is} + \frac{1}{I} \sum_{i=1}^{\infty} \frac{a_i s}{s^2 + 2\zeta_i \omega_i s + \omega_i^2} \quad (52)$$

$$\frac{y(s)}{T(s)} = P(s) = \frac{L}{Is^2} + \frac{1}{I} \sum_{i=1}^{\infty} \frac{k_i}{s^2 + 2\zeta_i \omega_i s + \omega_i^2} \quad (53)$$

A PD-feedback with a reference input v

$$V_{in}(t) = -K_P\theta(t) - K_D\dot{\theta}(t) + v(t) \quad (54)$$

is applied to the aforementioned experimental setup; PD gain K_P and K_D are experimentally chosen to make the system stable. Letting a desired trajectory of the tip position as

$$y_d(t) = \begin{cases} 0 & 0 \leq t \leq 2 \\ \frac{\pi L}{2} \{-f(t)^6 + 3f(t)^4 - 3f(t)^2 + 1\} & 2 \leq t \leq 3 \\ 0 & 3 \leq t \leq 5 \end{cases} \quad (55)$$

where $f(t) = 2(t - 2.5)$, conducted was an experiment to apply the scheme of iterative learning control given in Corollary 7 to update the reference input $v(t)$ with respect to the trajectory of the error $y(t) - y_d(t)$ without identifying the transfer function $G(s) = \mathcal{L}[y(t)]/\mathcal{L}[v(t)]$. The length of the time horizon for the experiment is chosen sufficiently long in view of the interval of the support of $y_d(t)$ and the decay time of the impulse response of $G(s)$ estimated by an experiment.

Fig. 5 and 6 show the input v_k and tip position y_k with y_d , respectively, for the number of iteration $k = 1$ and $k = 15$. Fig. 7 shows the tip deflection $w(L, t)$ with the tip position y_k for $k = 15$ (Nishiki (2004)).

5. CONCLUSION

This paper proposed an algebraic expression of noncausal stable inversion based on the two-sided Laplace transform, which is classic but has not been used very much. It was shown that this simple expression brings an advantage that computing of stable inversion is reduced to simulation of the response of the plant and the reverse of the time

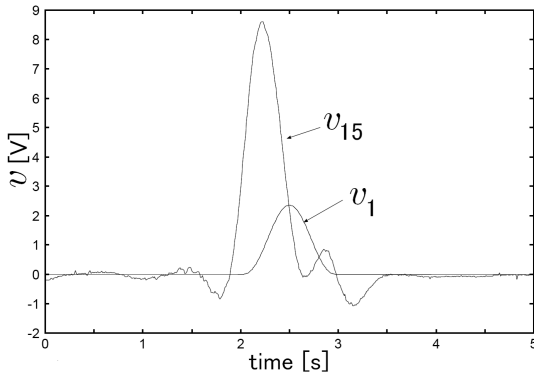


Fig. 5. Input profiles for $k = 1$ and $k = 15$

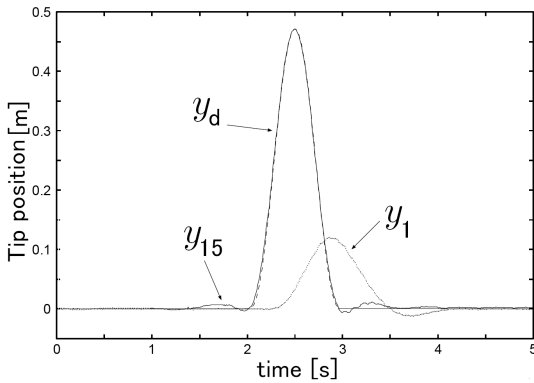


Fig. 6. Output for $k = 1$ and $k = 15$ with the desired trajectory

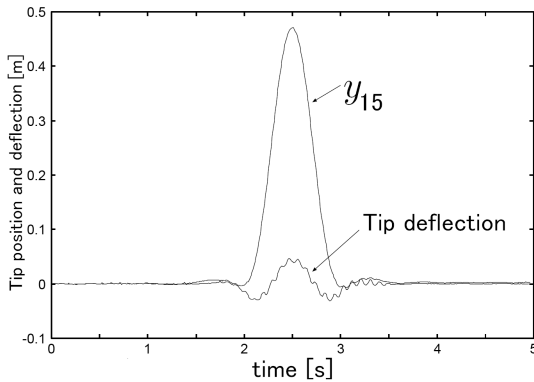


Fig. 7. Output with the tip deflection for $k = 15$

horizon without solving the boundary value problem as the conventional definition of stable inversion. An illustrative example demonstrates that this approach is useful for a search algorithm to choose a transition trajectory for the case where there is an input saturation. Moreover, algebraic expression extended the application class of stable inversion into infinite dimensional systems. A practical iterative method to obtain stable inversion for such systems was proposed. An experiment to apply the method to tip control of a flexible arm was presented.

Application of the aforementioned idea to discrete-time or sampled-data systems is straightforward by introducing the two-sided z-transform. This helps us to clarify a relation between inversion of sampled-data and continuous-time systems, the former of which mostly has unstable zeros even if the latter has no unstable zero. In another pa-

per, the author shows that the former with a small sample time actually approximates the latter (Sogo (2008)).

ACKNOWLEDGEMENTS

The author is grateful to Masakazu Nishiki for his help to conduct the experiment.

REFERENCES

- Robert H. Cannon and Eric Schmitz. Initial experiments on the end-point control of a flexible one-link robot. *The International Journal of Robotics Research*, 3(3):62–75, 1984.
- S. Devasia, D. Chen, and B. Paden. Nonlinear inversion-based output tracking. *IEEE Transactions on Automatic Control*, 41(7):930–942, 1996.
- L. R. Hunt, G. Meyer, and R. Su. Noncausal inverses for linear systems. *IEEE Transactions on Automatic Control*, 41(4):608–611, 1996.
- B. O. Kachanov and K. B. Khrolovich. Method for identification of dynamic systems with delays. *Automation and Remote Control*, 54(1):60–64, 1993.
- K. Kinoshita, T. Sogo, and N. Adachi. Iterative learning control using adjoint systems and stable inversion. *Asian Journal of Control*, 4(1):60–67, 2002.
- D. J. N. Limebeer, E. M. Kasenally, and J. D. Perkins. On the design of robust two degree of freedom controllers. *Automatica*, 29(1):157–168, 1993.
- O. Markusson, H. Hjalmarsson, and M. Norrlöf. Iterative learning control of nonlinear non-minimum phase systems and its application to system and model inversion. *Proc of the 40th IEEE Conference on Decision and Control*, 2001.
- K. L. Moore. *Iterative Learning Control for Deterministic Systems*. Springer-Verlag, 1993.
- M. Nishiki. Iterative learning control using input-output data for linear nonminimum phase systems. *Master's thesis at the graduate school of informatics, Kyoto University*, 2004. (in Japanese).
- D. H. Owens and J. Hätönen. Iterative learning control—an optimization paradigm. *Annual Reviews in Control*, 29: 57–70, 2005.
- A. Papoulis. *The Fourier Integral and Its Applications*. McGraw-Hill, 1962.
- A. Piazzoli and A. Visioli. Using stable input-output inversion for minimum-time feedforward constrained regulation of scalar systems. *Automatica*, 41(2):305–313, 2005.
- L. M. Silverman. Inversion of multivariable linear systems. *IEEE Transactions on Automatic Control*, AC-14(3): 270–276, 1969.
- T. Sogo. Inversion of sampled-data system approximates the continuous-time counterpart in a noncausal framework. *Automatica*, 44(3):823–829, 2008.
- B. Van der Pol and H. Bremmer. *Operational Calculus based on the Two-sided Laplace Integral*. Chelsea Publishing Company, 1987.
- Q. Zou and S. Devasia. Preview-based stable-inversion for output tracking of linear systems. *ASME Journal of Dynamic Systems, Measurement, and Control*, 121: 625–630, 1999.